Immobilization of Lanthanide Ions in a Pillared Layered Double Hydroxide

Sandra Gago,[†] Martyn Pillinger,*[,†] Rute A. Sá Ferreira,[‡] Luís D. Carlos,[‡] Teresa M. Santos,[†] and Isabel S. Gonçalves*[,†]

Departments of Chemistry and Physics, CICECO, University of Aveiro, 3810-193 Aveiro, Portugal

Received July 1, 2005

A Zn−Al layered double hydroxide (LDH) pillared by 2,2′-bipyridine-5,5′-dicarboxylate (BDC) anions was used as a porous matrix to intercalate $LnCl_3$ (Ln = Eu, Gd). Metal loadings of 9.0 wt % for Eu and 11 wt % for Gd were achieved, which correspond to about two lanthanide ions for every three BDC ions. The fitting of the room-temperature Eu L_3-edge EXAFS for the europium-containing material revealed one shell of 7 ± 1 oxygen/nitrogen atoms at 2.41 Å. No evidence for a Eu−Cl bond was found. The emission spectra for this material display the typical Eu^{3+} red emission and a large broad band peaking around 460 nm, which was attributed to the emission arising from the triplet levels of free ligands not coordinated to Eu^{3+} ions. Measurement of the emission spectra under different excitation wavelengths and also at low temperature showed the existence of only one type of Eu^{3+} binding site. The $^5D_0$ quantum efficiency was estimated to be low (7.7%), due to a relatively high nonradiative transition probability caused by the presence of water molecules in the first coordination shell. The number of water molecules was calculated as 3.6 ± 1, suggesting that the incorporated europium ions were 6-coordinate with four oxygen atoms from water molecules and two nitrogen atoms from a bidentate bipyridyl ligand.

Introduction

In recent years, layered double hydroxides (LDHs) have been investigated for numerous applications, mainly due to their unique anion-exchange properties.[1] The structure of these materials is derived from that of brucite, which consists of $Mg(OH)_6$ octahedral units sharing edges to form $Mg(OH)_2$ slabs. In LDHs, isomorphous replacement of some of the Mg^{2+} cations by M^{3+} cations, such as Al^{3+} and Ga^{3+}, gives positively charged layers. The charge is compensated by the intercalation of an appropriate number of anions into the interlayer region. There are also interlayer water molecules which hydrogen-bond with the layer hydroxyl groups and sometimes also with the charge-balancing anions. Materials containing divalent metal cations other than Mg^{2+} also exist, e.g., Co^{2+}, Ni^{2+}, and Zn^{2+}. The general formula can be written as $[M^{2+}_{1-x}M^{3+}_x(OH)_2]A^{m-}_{x/m}\cdot nH_2O$. A large number of organic and inorganic anions have been intercalated by direct synthesis, ion exchange, or reconstruction of the layered structure when contacting a precursor material calcined at 573−773 K with solutions of anions.[2,3] Materials containing metallo-organic species, mainly oxalate complexes, cyanocomplexes, phthalocyanines, and porphyrins, have also been prepared.[3] These hybrid materials find use as catalytic, photoactive, and electroactive materials. Intercalation of a complex into the interlayer space can dramatically influence the properties of both the guest and the host.

LDHs containing metal complexes of chelating ligands, mainly nitrilotriacetate (NTA) and EDTA (ethylenediaminetetraacetate), have also been prepared, either directly by intercalation of the metal complex or indirectly by forming the metal complex between the host layers following intercalation of the ligand.[4,5] One of these reports describes the uptake of La^{3+} and NO_3^- ions by an NTA-intercalated Mg−Al LDH to form chelate complexes within the layer.[5] In general, materials which embed lanthanide chelate complexes are of interest because they have the potential to be used in optoelectronic devices.[6] So far, concerning LDHs, the incorporation of $Eu(EDTA)^-$ and $Eu(pic)_4^-$ (pic = picolinate) complexes into Mg−Al materials has been studied.[7] We recently reported the synthesis and characterization of a Zn−Al LDH pillared by 2,2′-bipyridine-5,5′-

* To whom the correspondence should be addressed. M.P.: (tel) 00351-234-378123; (fax) 00351-234-370084; (e-mail) mpillinger@dq.ua.pt. I.S.G.: (tel) 00351-234-378190; (fax) 00351-234-370084; (e-mail) igoncalves@dq.ua.pt.

[†] Department of Chemistry.

[‡] Department of Physics.

(1) *Layered Double Hydroxides: Present and Future*; Rives, V., Ed.; Nova Science Publishers: New York, 2001.

(2) Khan, A. I.; O'Hare, D. *J. Mater. Chem.* **2002**, *12*, 3191. Newman, S. P.; Jones, W. *New J. Chem.* **1998**, *22*, 105.

(3) Rives, V.; Ulibarri, M. A. *Coord. Chem. Rev.* **1999**, *181*, 61.

(4) Tarasov, K. A.; O'Hare, D.; Isupov, V. P. *Inorg. Chem.* **2003**, *42*, 1919. Tsyganok, A. I.; Suzuki, K.; Hamakawa, S.; Takehira, K.; Hayakawa, T. *Chem. Lett.* **2001**, 24. Tarasov, K. A.; Isupov, V. P.; Chupakhina, L. E. *Russ. J. Inorg. Chem.* **2000**, *45*, 1659. Gutmann, N. H.; Spiccia, L.; Turney, T. W. *J. Mater. Chem.* **2000**, *10*, 1219. Kaneyoshi, M.; Jones, W. *J. Mater. Chem.* **1999**, *9*, 805.

(5) Kaneyoshi, M.; Jones, W. *Mol. Cryst. Liq. Cryst.* **2001**, *356*, 459.

(6) See for example Rocha, J.; Carlos, L. D. *Curr. Opin. Solid State Mater. Sci.* **2003**, *7*, 199. Maas, H.; Currao, A.; Calzaferri, G. *Angew. Chem., Int. Ed.* **2002**, *41*, 2495. Sendor, D.; Kynast, U. *Adv. Mater.* **2002**, *14*, 1570. Li, H. R.; Lin, J.; Zhang, H. J.; Fu, L. S.; Meng, Q. G.; Wang, S. B. *Chem. Mater.* **2002**, *14*, 3651. Alvaro, M.; Fornés, V.; García, S.; Garcia, H.; Scaiano, J. C. *J. Phys. Chem. B* **1998**, *102*, 8744. Brunet, E.; de la Mata, M. J.; Juanes, O.; Rodríguez-Ubis, J. C. *Chem. Mater.* **2004**, *16*, 1517. Ferreira, R.; Pires, P.; de Castro, B.; Sá Ferreira, R. A.; Carlos, L. D.; Pischel, U. *New J. Chem.* **2004**, *28*, 1506.

(7) Li, C.; Wang, G.; Evans, D. G.; Duan, X. *J. Solid State Chem.* **2004**, *177*, 4569. Zhuravleva, N. G.; Eliseev, A. A.; Lukashin, A. V.; Kynast, U.; Tret'yakov, Y. D. *Dokl. Chem.* **2004**, *396*, 87.

10.1021/cm051431p CCC: $30.25
Published on Web 10/15/2005

dicarboxylate (BDC) anions.[8] The material was examined as a "solid ligand" for the immobilization of the dioxomolybdenum(VI) complex $MoO_2Cl_2(THF)_2$, giving a stable heterogeneous catalyst for the liquid-phase epoxidation of olefins. In the present work, the Zn−Al LDH pillared by BDC anions has been examined as a solid-state complexation material for europium(III) and gadolinium(III) ions. The resultant organic−inorganic hybrid composites have been characterized by elemental analysis, powder XRD, TGA, FTIR and FT Raman spectroscopy, X-ray absorption fine structure spectroscopy, and photoluminescence spectroscopy.

Experimental Section

Characterization Methods. Microanalyses for CHN were carried out at the Instituto de Tecnologia Química e Biológica, Oeiras (by C. Almeida). Zn, Al, Eu, and Gd were determined by ICP-AES at the Central Laboratory for Analysis, University of Aveiro (by E. Soares). Powder X-ray diffraction (XRD) data were collected at room temperature on a Philips X'pert diffractometer with a curved graphite monochromator (Cu Kα radiation), in a Bragg−Brentano para-focusing optics configuration. Samples were step-scanned in 0.02° 2θ steps with a counting time of 2 s per step. Thermogravimetric analysis (TGA) was performed using a Shimadzu TGA-50 system at a heating rate of 5 °C min^{-1} under air. IR spectra were measured on a Mattson 7000 FT-IR spectrometer using KBr pellets. Raman spectra were recorded on a Bruker RFS100/S FT instrument (Nd:YAG laser, 1064 nm excitation and InGaAs detector). Solid-state NMR spectra were measured at 100.62 MHz for ^{13}C and 104.26 MHz for ^{27}Al with a (9.4 T) wide bore Bruker Avance 400 spectrometer. ^{13}C CP MAS NMR spectra were acquired with a 3.5 μs 90° proton pulse and 2 ms contact time with spinning rates of 7−8.5 kHz and 4 s recycle delays. Chemical shifts are quoted in ppm from TMS. Single-quantum ("conventional") ^{27}Al MAS NMR spectra were acquired using short and powerful radio frequency pulses (0.6 μs, corresponding to $\pi/12$ pulses), a spinning rate of 14 kHz, and a recycle delay of 1 s. Chemical shifts are quoted in ppm from $Al(H_2O)_6^{3+}$.

Eu L_3-edge X-ray absorption spectra were measured in transmission mode on beamline BM29 at the ESRF (Grenoble),[9] operating at 6 GeV in hybrid mode with typical currents of 170−190 mA. The low-temperature spectra were recorded using an Oxford Instruments cryostat filled with He exchange gas. Scans were set up to record the pre-edge at 5 eV steps and the post-edge region in 0.025−0.05 $Å^{-1}$ steps, giving a total acquisition time of ca. 30 min per scan. The order-sorting double Si(311) crystal monochromator was detuned by 50% for harmonic rejection. Solid samples were diluted with BN and pressed into 13 mm pellets. Ionization chamber detectors were filled with N_2 to give 30% absorbing I_o (incidence) and 70% absorbing I_t (transmission). The programs EXCALIB and EXBACK (SRS Daresbury Laboratory, UK) were used in the usual manner for calibration and background subtraction of the raw data. EXAFS curve-fitting analyses, by least-squares refinement of the non-Fourier filtered k^3-weighted EXAFS data, were carried out using the program EXCURVE (version EXCURV98[10]) using fast curved wave theory.[11] The calculations were performed with single scattering contributions only. Phase shifts were obtained within this program using ab initio calculations based on the Hedin Lundqvist/von Barth scheme. For each EXAFS simulation the validity of extra parameters was checked using a comparative reduced χ^2 method.[12]

The room-temperature photoluminescence and lifetime measurements were recorded on a modular double grating excitation spectrofluorimeter with a TRIAX 320 emission monochromator (Fluorolog-3, Jobin Yvon-Spex) coupled to a R928 Hamamatsu photomultiplier, using front face acquisition mode. All of the spectra were corrected for optics and detection spectral response.

Materials. The lanthanide trichloride hexahydrates $LnCl_3 \cdot 6H_2O$ (Ln = Eu, Gd) were obtained from Aldrich and used as received. Literature methods were used to prepare the complex $[(bipy)Eu(OH_2)_4Cl_2]Cl \cdot H_2O$ (**1**) (bipy = 2,2′-bipyridine)[13] and a Zn−Al LDH with the composition $Zn_{2.9}Al_2(OH)_{9.8}(BDC) \cdot 7H_2O$ (BDC = 2,2′-bipyridine-5,5′-dicarboxylate), designated as Zn−Al−BDC.[8]

Zn−Al−BDC/Eu. A solution of $EuCl_3 \cdot 6H_2O$ (0.2 g, 0.55 mmol) in decarbonated deionized (DD) water (40 mL) was stirred for 15 min at 80 °C and added dropwise to an aqueous suspension of Zn−Al−BDC (0.35 g). The mixture was stirred under reflux for 6 h. The solid was recovered by centrifugation, washed several times with warm DD water, and dried under vacuum. Anal. Calcd for $Zn_{3.1}Al_2(OH)_{10.2}(BDC)(EuCl_3)_{0.65} \cdot 14H_2O$: Zn, 18.56; Al, 4.94; Eu, 9.04; C, 13.19; N, 2.56; H, 4.08. Found: Zn, 18.60; Al, 4.98; Eu, 9.00; C, 14.01; N, 2.44; H, 3.14. IR (KBr, cm^{-1}): 3415 (br), 1614 (vs), 1595 (sh), 1556 (m), 1473 (w), 1397 (sh), 1381 (vs), 1303 (w), 1258 (w), 1213 (w), 1162 (w), 1129 (w), 1037 (m), 1008 (w), 951 (sh), 841 (m), 775 (m), 734 (w), 709 (w), 669 (w), 618 (m), 577 (m), 426 (vs), 400 (sh), 325 (w). Raman (cm^{-1}): 3088, 3065, 1602, 1495, 1418 (sh), 1406, 1379, 1362, 1320, 1282, 1263, 1237, 1172, 1145, 1040, 873, 808, 675, 650, 312, 145. ^{13}C CP MAS NMR: δ 120.2, 140.9, 148.6 (all bipy-C), 168.0 ($C-CO_2^-$) ppm. ^{27}Al MAS NMR: δ 15.2 ppm.

Zn−Al−BDC/Gd. A solution of $GdCl_3 \cdot 6H_2O$ (0.26 g, 0.7 mmol) in ethanol (10 mL) was added dropwise to a suspension of Zn−Al−BDC (0.5 g) in ethanol. The mixture was stirred for 18 h at room temperature. The solid was recovered by filtration, washed several times with ethanol, and dried under vacuum. Anal. Calcd for $Zn_{2.8}Al_2(OH)_{9.6}(BDC)(GdCl_3)_{0.68} \cdot 9H_2O$: Zn, 18.61; Al, 5.48; Gd, 10.87; C, 14.65; N, 2.85; H, 3.44. Found: Zn, 18.40; Al, 5.49; Gd, 11.00; C, 15.13; N, 2.70; H, 3.24. IR (KBr, cm^{-1}): 3400 (br), 1614 (vs), 1593 (sh), 1556 (m), 1473 (w), 1405 (sh), 1382 (vs), 1304 (w), 1259 (w), 1226 (sh), 1163 (w), 1136 (w), 1038 (m), 960 (sh), 871 (sh), 841 (w), 808 (sh), 777 (m), 710 (w), 666 (w), 620 (m), 561 (m), 425 (s), 325 (w). Raman (cm^{-1}): 3080, 1599, 1493, 1428 (sh), 1403, 1361, 1318, 1288, 1262, 1170, 1146, 1041, 862, 808, 673, 649, 553, 417, 312, 158, 108.

Results and Discussion

The pillared LDH Zn−Al−BDC, with a Zn/Al molar ratio of 1.45 and containing ca. 1.3 mmol of 2,2′-bipyridine-5,5′-dicarboxylate anions per gram of material, was treated with solutions of $LnCl_3 \cdot 6H_2O$ (Ln = Eu, Gd) in 10−20% excess over that required for a 1:1 $LnCl_3$/BDC stoichiometry. Elemental analysis of the final materials Zn−Al−BDC/Ln showed the incorporation of approximately two lanthanide cations for every three BDC anions. The Zn/Al molar ratios

(8) Gago, S.; Pillinger, M.; Valente, A. A.; Santos, T. M.; Rocha, J.; Gonçalves, I. S. *Inorg. Chem.* **2004**, *43*, 5422.
(9) Filipponi, A.; Borowski, M.; Bowron, D. T.; Ansell, S.; Cicco, A. D.; Panfilis, S. D.; Itiè, J.-P. *Rev.-Sci. Instrum.* **2000**, *71*, 2422.
(10) Binsted, N. EXCURV98, CCLRC Daresbury Laboratory computer program, 1998.
(11) Gurman, S. J.; Binsted, N.; Ross, I. *J. Phys. C* **1984**, *17*, 143. Gurman, S. J.; Binsted, N.; Ross, I. *J. Phys. C* **1986**, *19*, 1845.
(12) O'Donnell, K. P.; Mosselmans, J. F. W.; Martin, R. W.; Pereira, S.; White, M. E. *J. Phys.: Condens. Matter* **2001**, *13*, 6977.
(13) Semenova, L. I.; Skelton, B. W.; White, A. H. *Aust. J. Chem.* **1999**, *52*, 551.

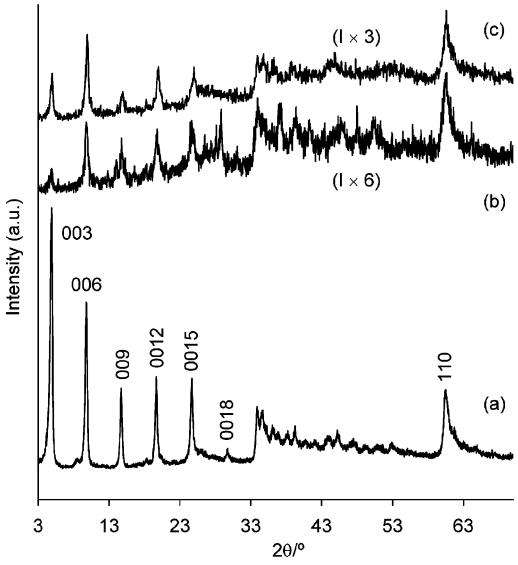

Figure 1. Powder XRD patterns of (a) Zn−Al−BDC, (b) Zn−Al−BDC/Eu, and (c) Zn−Al−BDC/Gd.

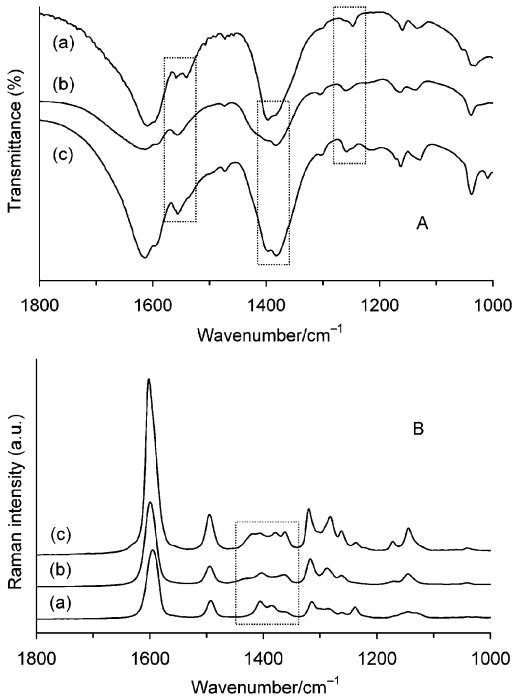

Figure 2. FTIR (A) and FT Raman (B) spectra in the range 1000−1800 cm^{-1} for (a) Zn−Al−BDC, (b) Zn−Al−BDC/Gd, and (c) Zn−Al−BDC/Eu. The changes upon incorporation of the lanthanide ions are highlighted with boxes.

were unaffected by the treatment and there was no indication that BDC ions were exchanged for chloride ions. Figure 1 shows the powder XRD patterns for Zn−Al−BDC, Zn−Al−BDC/Eu, and Zn−Al−BDC/Gd at ambient temperature in the range of 3−70° 2θ. The basal (003) reflection for Zn−Al−BDC appears at 18.0 Å and a further 5 equally spaced 00l harmonics are observed up to 30° 2θ. As described previously,[8] the basal spacing is consistent with a model in which the BDC anions are arranged with their longest dimension nearly perpendicular to the host layers. Upon treatment with $LnCl_3$, the 00l reflections are essentially unshifted but significantly reduced in intensity. The first-order peak is weaker than the second-order peak for Zn−Al−BDC/Ln, in contrast to that observed for Zn−Al−BDC.

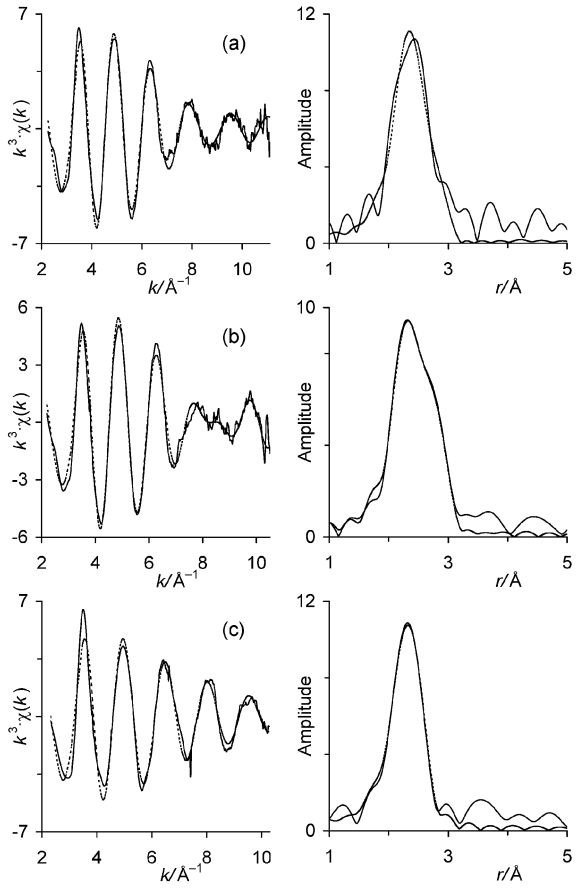

Figure 3. Room-temperature Eu L_3-edge EXAFS and Fourier transforms of (a) $EuCl_3 \cdot 6H_2O$, (b) $[(bipy)Eu(OH_2)_4Cl_2]Cl \cdot H_2O$ (**1**), and (c) Zn−Al−BDC/Eu. The solid line represents the experimental data and the dashed line shows the best fit using parameters given in Table 1.

These changes can be attributed to a marked increase in the electron density at the midpoint of the interlayers due to the presence of the rare earth ions at a high loading (9−11 wt %).[14]

The LDH materials were also characterized by IR and Raman spectroscopy. In the frequency range 4000−2000 cm^{-1}, the IR spectrum of Zn−Al−BDC is dominated by a broad band at about 3410 cm^{-1}, attributed to the O−H stretch of weakly hydrogen-bonded water molecules and layer hydroxyl groups. A band for the C−H stretch of the bipyridine (bipy) rings is observed in the Raman spectrum at about 3080 cm^{-1}. In this high-frequency region, the IR and Raman spectra for the final materials Zn−Al−BDC/Ln are not very different from those of the precursor pillared LDH. Some changes were, however, observed in the region between 1800 and 1000 cm^{-1}, which contains the vibrations of the bipy framework and the carboxylate groups (Figure 2). The absence of IR bands above 1650 cm^{-1} in the spectrum of Zn−Al−BDC indicates that there are no acid C═O bonds present. Instead, there is an intense, broad band at 1609 cm^{-1} (overlapping the highest bipy band), which is assigned to the antisymmetric stretch of CO_2^-. The other intense band in this spectrum at 1397 cm^{-1} (shoulder at 1383 cm^{-1}) is assigned as the symmetric stretch of CO_2^-. The bands for the bipy in-plane ring stretching modes (with

(14) Beaudot, P.; de Roy, M. E.; Besse, J. P. *Chem. Mater.* **2004**, *16*, 935.

Table 1. Eu L_3-Edge EXAFS-Derived Structural Parameters for Model Compounds and the Hybrid LDH Zn−Al−BDC/Eu

compound	atom	CN[a]	r/Å	$2\sigma^2$/Å^{2b}	E_f/eV[c]	R (%)[d]
$EuCl_3 \cdot 6H_2O$, 298 K	O	6.5(3)	2.427(4)	0.0187(9)	−8.6(3)	20.0
	Cl	2.1(5)	2.765(9)	0.0241(22)		
$EuCl_3 \cdot 6H_2O$, 20 K	O	6.6(4)	2.423(5)	0.0107(8)	−8.6(4)	24.2
	Cl	2.1(6)	2.771(10)	0.0167(22)		
$[(bipy)Eu(OH_2)_4Cl_2]Cl \cdot H_2O$, 298 K	O	5.3(3)	2.425(4)	0.0160(8)	−9.6(3)	19.0
	Cl	2.1(3)	2.776(5)	0.0134(10)		
$[(bipy)Eu(OH_2)_4Cl_2]Cl \cdot H_2O$, 20 K	O	6.1(3)	2.417(3)	0.0101(5)	−9.2(2)	18.6
	Cl	2.2(3)	2.770(4)	0.0103(8)		
	C	4.3(12)	3.567(20)	0.0240(64)		
Zn−Al−BDC/Eu, 298 K	O	6.9(4)	2.412(5)	0.0199(9)	−7.5(3)	21.2

[a] CN = coordination number. Values in parentheses are statistical errors generated in EXCURVE. The true errors in coordination numbers are likely to be of the order of 20% and those for the interatomic distances ca. 1.5%.[17] [b] Debye−Waller factor; σ = root-mean-square internuclear separation. [c] E_f = edge position (Fermi energy), relative to calculated vacuum zero. [d] $R = (\int[\Sigma^{theory} - \Sigma^{exptl}]k^3 dk / [\Sigma^{exptl}]k^3 dk) \times 100\%$.

contributions from C−H in-plane bending and ring−ring stretching) are observed at 1597, 1558, 1540, 1472, 1302, and 1247 cm^{-1} (shoulder at 1258 cm^{-1}) in the IR and at 1595, 1493, 1405, 1362, 1314, 1286, and 1262 cm^{-1} in the Raman. Upon incorporation of the lanthanide ions, some marked differences can be observed in terms of the number of bands in the 1800−1000 cm^{-1} range. For example, instead of two IR bands at 1558 and 1540 cm^{-1}, only one band is observed for Zn−Al−BDC/Eu and Zn−Al−BDC/Gd at 1556 cm^{-1}. In the Raman spectrum of Zn−Al−BDC/Eu, a new band is present as a shoulder at 1418 cm^{-1} (1428 cm^{-1} for Zn−Al−BDC/Gd). Some significant changes are also apparent in the relative intensities of the IR bands at ca. 1400/1382 and 1258/1247 cm^{-1}. These alterations in the vibrational spectra can be tentatively interpreted as evidence of a Ln^{3+}−N(bipy) interaction. On the other hand, the stretching vibrations for the carboxylate groups are unshifted, which suggests that there is no interaction between these functional groups and the lanthanide ions.

Below 1000 cm^{-1}, the IR spectra of the LDH materials contain some bands due to the guest species in addition to peaks arising from the host lattice. No significant changes were observed in this region upon incorporation of the lanthanide ions. A relatively sharp band at 776 cm^{-1} is assigned to C−H out-of-plane bending, and a broad band at about 620 cm^{-1} is due either to a librational mode of hydroxyl groups and water or to a metal−oxygen vibration ν(M−O) (M = Zn, Al).[15] Two peaks at about 560 and 426 cm^{-1} are attributed to ν(M−O) and δ(M−O−M), respectively.

Eu L_3-edge EXAFS studies were carried out in the solid state in order to characterize the average local coordination environment of europium centers in Zn−Al−BDC/Eu. Europium chloride hexahydrate, $EuCl_3 \cdot 6H_2O$, and the adduct $[(bipy)Eu(OH_2)_4Cl_2]Cl \cdot H_2O$ (**1**) were measured as model compounds. A single-crystal X-ray structural analysis of $EuCl_3 \cdot 6H_2O$ showed that the structure consists of the "complex" ions $[Eu(H_2O)_6Cl_2]^+$ and "isolated" Cl^- ions.[16] The average of the Eu−H_2O distances was determined as 2.44 ± 0.6 Å and the Eu−Cl distance was 2.76 Å. A two shell fit to the k^3-weighted room-temperature EXAFS of $EuCl_3 \cdot 6H_2O$ gave 6.5 oxygens at 2.43 Å and 2.1 chlorines at 2.77 Å, in good agreement with the crystal values (Figure 3, Table 1). Crystallographic studies showed that the first shell coordination environment of europium in the adduct **1** is not very different from that in europium chloride hexahydrate, except that two oxygen atoms from water molecules are replaced by two nitrogen atoms from the bipyridine ligand (r_{Eu-O} = 2.42 ± 0.3 Å, r_{Eu-N} = 2.55 Å, r_{Eu-Cl} = 2.723, 2.776 Å).[13] A good fit to the room-temperature $k^3 \cdot \chi(k)$ data was obtained with 5.3 oxygen atoms at 2.43 Å and 2.1 chlorines at 2.78 Å. We could not discriminate between oxygen and nitrogen atoms as possible nearest neighbors for Eu because their backscattering amplitudes and phases are very similar. However, for the EXAFS recorded at low temperature (20 K), it was possible to add a third shell for carbon atoms at 3.57 Å (Table 1). This shell was statistically significant as measured by the reduced χ^2 test. However, the $r_{Eu}\cdots C$ distance is about 0.1 Å longer than expected. The room-temperature EXAFS of Zn−Al−BDC/Eu was best modeled by a one shell fit comprising 6.9 oxygen atoms at 2.41 Å. It was not possible to satisfactorily fit Eu−Cl correlations using a second shell. Also, for the reasons stated above, we could neither rule in nor rule out the presence of nitrogen backscatterers in the first shell. Recording the EXAFS at lower temperature did not reveal the presence of Eu···C or Eu···Eu correlations. This means that if such correlations exist, they must be very disordered and their contribution to the EXAFS, therefore, is below the level of statistical noise.

As might be expected from the EXAFS results, the compounds $[(bipy)Eu(OH_2)_4Cl_2]Cl \cdot H_2O$ (**1**) and Zn−Al−BDC/Eu have very different photoluminescence properties. We will first describe the photophysical characterization of the model complex. The excitation spectrum of complex **1**, monitored within the intra-4f^6 $^5D_0 \rightarrow {}^7F_2$ lines, is composed of a large broad band, with two main components in the ultraviolet (UV) spectral region peaking around 300 and 335 nm, and a series of sharp lines ascribed to the typical Eu^{3+} intra-4f^6 transitions (Figure 4). The large broad band may result from the energy levels of the ligand(s) and/or from a charge transfer state. The intensity of the Eu^{3+} lines is closer to that of the large broad band, indicating that the excitation of the metal ion occurs both through direct lanthanide excitation and via a sensitized process involving the lanthanide ion ligands.

(15) Kagunya, W.; Baddour-Hadjean, R.; Kooli, F.; Jones, W. *Chem. Phys.* **1998**, *236*, 225. Kloprogge, J. T.; Frost, R. L. In *Layered Double Hydroxides: Present and Future*; Rives, V., Ed.; Nova Science Publishers: New York, 2001; pp 139−192.

(16) Bel'skii, N. K.; Struchkov, Y. T. *Sov. Phys. Crystallogr.* **1965**, *10*, 15.

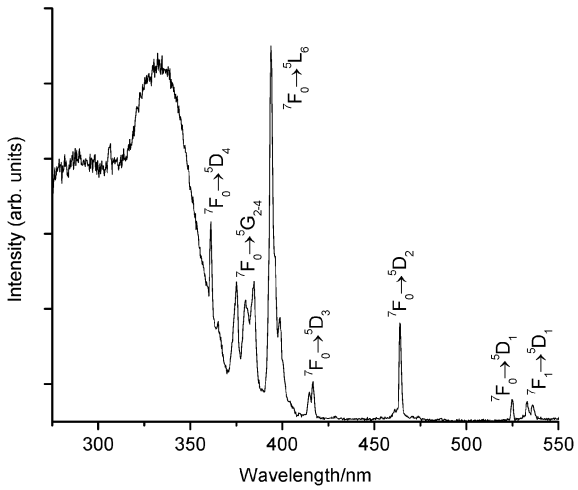

Figure 4. Excitation spectrum monitored around 612 nm for the model complex $[(bipy)Eu(OH_2)_4Cl_2]Cl\cdot H_2O$ (**1**).

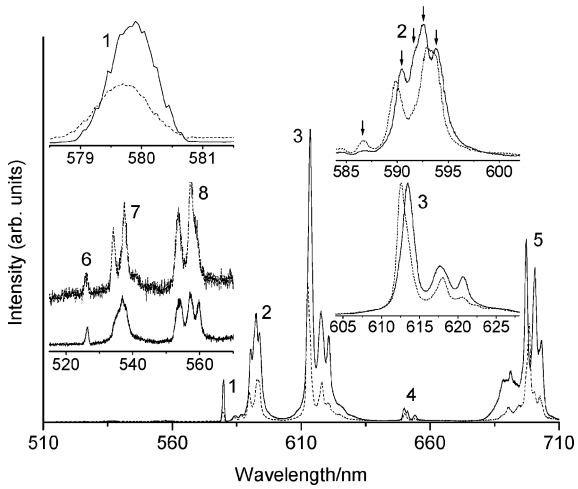

Figure 5. Emission spectra excited around 344 nm (solid line) and 395 nm (dashed line) for $[(bipy)Eu(OH_2)_4Cl_2]Cl\cdot H_2O$ (**1**). (1), (2), (3), (4), and (5) denote the $^5D_0 \rightarrow {}^7F_{0-4}$ transitions and (6), (7), and (8) denote the $^5D_1 \rightarrow {}^7F_{0-2}$ transitions.

Table 2. $^5D_0$ Lifetime Values (ms) Monitored around 612 nm at Different Excitation Wavelengths for the Complex $[(bipy)Eu(OH_2)_4Cl_2]Cl\cdot H_2O$ (1) and the Material Zn−Al−BDC/Eu

	excitation wavelength (nm)	
compound	344−354	395
1	0.155 ± 0.001	0.129 ± 0.001
Zn−Al−BDC/Eu	0.195 ± 0.002	0.199 ± 0.004

The emission features of the model complex **1** were investigated under different excitation wavelengths: (i) within the large broad band and (ii) directly in the Eu^{3+} levels ($^5L_6$, 395 nm). The spectra are composed of emission lines ascribed to transitions from the first ($^5D_0$) and second ($^5D_1$) excited states of the metal ions, and no emission arising from the ligand triplet levels could be detected, suggesting an efficient energy transfer between the ligands and the Eu^{3+} ions (Figure 5). For direct excitation into the $^5L_6$ level, at least 5 Stark components can be discerned for the $^5D_0 \rightarrow {}^7F_1$ transition (marked with arrows in Figure 5). The maximum splitting ($2J + 1$) for this transition is 3 Stark components, and hence there are at least two different Eu^{3+} local coordination sites. Moreover, upon decreasing of the excitation wavelength, changes in the relative intensity and

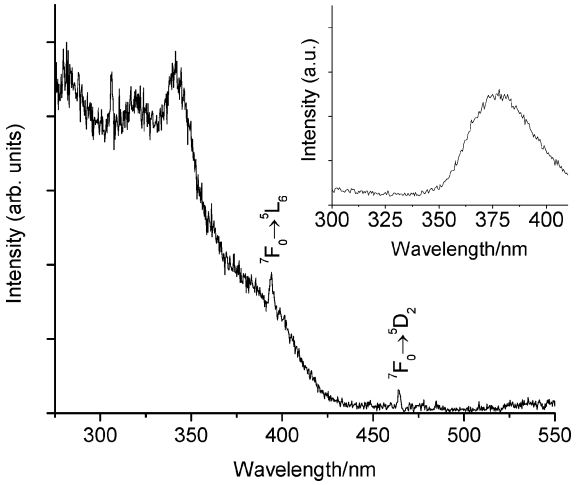

Figure 6. Excitation spectrum monitored around 612 nm for Zn−Al−BDC/Eu. The inset shows the excitation spectrum of Zn−Al−BDC/Gd, monitored around 438 nm.

energy of the emission lines are observed. In particular, the $^5D_0 \rightarrow {}^7F_0$ transition undergoes a red-shift (6 cm^{-1}). Since this transition occurs between non-degenerated states, the presence of more than one line or changes in their energy as the excitation wavelength is varied unequivocally suggest the presence of more than one type of coordination sphere for the metal ion. The lifetimes of the $^5D_0$ level were monitored around the $^5D_0 \rightarrow {}^7F_2$ transition for the excitation wavelengths used to record the emission spectra. All of the decay curves present a typical single-exponential behavior, revealing lifetime values that depend on the selected excitation wavelength (Table 2), which is compatible with the presence of at least two different Eu^{3+} coordination sites in complex **1**. This is in disagreement with the single-crystal X-ray study of **1**, where only one type of europium atom was found.[13] Two possibilities are that either complex **1** has two Eu^{3+} sites with slightly different local coordination spheres or the synthesized compound has a Eu-based impurity. The existence of two similar Eu^{3+} sites is unlikely considering the clear changes observed in the local-field splitting of the $^7F_{1,2}$ levels as the excitation energy was varied (Figure 5). We therefore suggest the presence of a minor amount of a europium-based impurity in compound **1** (only detected by PL). Such a small amount is consistent with the minor changes in the monoexponential decay curves for different excitation energies (Table 2).

Figure 6 shows the excitation spectrum of the material Zn−Al−BDC/Eu monitored within the Eu^{3+} lines. The spectrum consists mainly of a large broad band showing at least three components centered around 320, 340, and 375 nm, and of a series of intra-$4f^6$ lines. The relatively low intensity of the Eu^{3+} lines with respect to the main band indicates that the metal ions are excited essentially via a sensitized process, rather than by direct excitation into the Eu^{3+} levels.

To discern the nature of the large broad band in the excitation spectrum, the analysis of the photoluminescent features of the equivalent compound incorporating Gd^{3+} metal ions, rather than Eu^{3+}, is a useful tool because the energetic difference between the Gd^{3+} excited levels and the

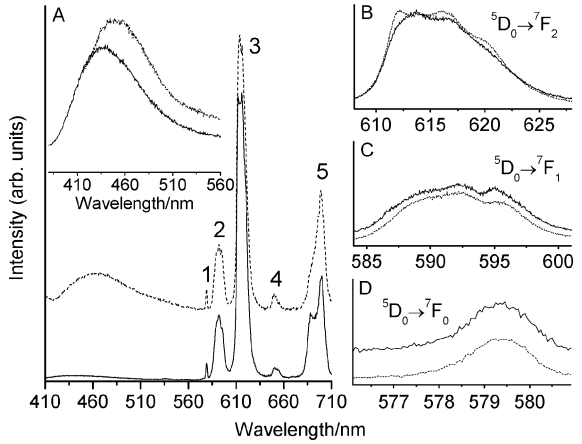

Figure 7. (A) Emission spectra excited around 354 nm (solid line) and 395 nm (dashed line) for Zn−Al−BDC/Eu. (1), (2), (3), (4), and (5) denote the $^5D_0 \rightarrow {}^7F_{0-4}$ transitions. The inset shows the emission spectra of Zn−Al−BDC/Gd for the same excitation wavelengths. (B), (C), and (D) show in detail the $^5D_0 \rightarrow {}^7F_{0-2}$ transitions.

ground state is much higher than those typical of ligand singlet and triplet states, disabling, therefore, any ligand-to-metal energy transfer process and allowing the charge transfer states and ligand levels to be distinguished. The spectrum of Zn−Al−BDC/Gd is composed of a large broad band centered at 365 nm, and no sign of UV components could be detected. Thus, it is possible to assign the UV components in the PLE spectra of Zn−Al−BDC/Eu to charge-transfer bands and the components at higher wavelengths may be ascribed to the ligand levels, in particular, the singlet state.

Figure 7 shows the emission spectra for the material Zn−Al−BDC/Eu obtained under different excitation wavelengths. The spectra display the typical Eu^{3+} red emission and a large broad band peaking around 460 nm. This band resembles that measured for the corresponding Gd-based compound (inset of Figure 7) and can therefore be attributed to the emission arising from the triplet levels of free ligands that are not coordinated to Eu^{3+} ions. The energy transfer between these free ligands and the metal ions is likely to be inefficient, resulting in the observation of the band in the emission spectrum. Analyzing in greater detail the Eu^{3+} emission lines plotted in Figure 7, it is clear that varying the excitation wavelength does not result in major changes to the lines, suggesting that all of the lanthanide ions occupy the same local coordination site. Moreover, upon lowering of the temperature, the spectra resemble those measured at room temperature, apart from an increase in the relative intensity of the emission band from the ligands with respect to the Eu^{3+} lines (not shown). The higher number of Stark components (3 and 4 for the $^5D_0 \rightarrow {}^7F_{1-2}$ transitions, respectively) and the higher intensity of the $^5D_0 \rightarrow {}^7F_2$ transition with respect to the magnetic dipole $^5D_0 \rightarrow {}^7F_1$ suggest that the local symmetry group around the metal ions has a low symmetry without an inversion center.

The presence of a single Eu^{3+} local environment is further confirmed by the measurement of the emission decay curve monitored around the $^5D_0 \rightarrow {}^7F_2$ transition for the excitation wavelengths used to record the emission spectra. All of the decay curves present a typical single-exponential behavior, revealing approximately the same lifetime value for the $^5D_0$ level, independent of the excitation wavelength (Table 2).

Based on the previous results, namely, emission and lifetime values of the $^5D_0$ level, we can estimate the efficiency, q, of the Eu^{3+} first-excited state. Assuming that only nonradiative and radiative processes are essentially involved in the depopulation of the $^5D_0$ state, q can be defined as

$$q = \frac{k_r}{k_r + k_{nr}} \tag{1}$$

where k_r and k_{nr} are the radiative and nonradiative transition probabilities, respectively (and k_{exp} (τ_{exp}^{-1}) is the experimental transition probability). The emission intensity, I, taken as the integrated intensity S of the emission lines for the $^5D_0 \rightarrow {}^7F_{0-6}$ transitions, is expressed by

$$I_{i\rightarrow j} = \hbar w_{i\rightarrow j} A_{i\rightarrow j} N_i \equiv S_{i\rightarrow j} \tag{2}$$

where i and j represent the initial ($^5D_0$) and final ($^7F_{0-4}$) levels, respectively, $\hbar w_{i\rightarrow j}$ is the transition energy, $A_{i\rightarrow j}$ is the Einstein coefficient of spontaneous emission, and N_i is the population of the $^5D_0$ emitting level.[18,19] As the $^5D_0 \rightarrow {}^7F_{5,6}$ transitions are not observed experimentally, we can ignore their influence on the depopulation of the $^5D_0$ excited state and therefore the radiative contribution is estimated based only on the relative intensities of the $^5D_0 \rightarrow {}^7F_{0-4}$ transitions. Since the $^5D_0 \rightarrow {}^7F_1$ transition can be considered as a reference, due to its dipolar magnetic nature, k_r can be calculated as

$$k_r = A_{0\rightarrow 1} \frac{\hbar\omega_{0\rightarrow 1}}{S_{0\rightarrow 1}} \sum_{J=0}^{4} \frac{S_{0-J}}{\hbar\omega_{0-J}} \tag{3}$$

where A_{0-1} is the Einstein coefficient of spontaneous emission between the $^5D_0$ and the $^7F_1$ Stark levels. The $^5D_0 \rightarrow {}^7F_1$ transition does not depend on the local ligand field seen by Eu^{3+} ions and can therefore be used as a reference for the whole spectrum, in vacuo $A_{0-1} = 14.65$ s^{-1}.[19] An average index of refraction of 1.5 was considered for both compounds leading to $A_{0-1} \approx 50$ s^{-1}. It was not possible to evaluate the q, k_r, and k_{nr} values for each local environment in the complex $[(bipy)Eu(OH_2)_4Cl_2]Cl\cdot H_2O$ (**1**), due to the presence of more than one local coordination site for the metal ions. Since it was not possible to selectively excite the emission ascribed to each Eu^{3+} ion, the emission intensity, I, cannot be determined independently, thus preventing any $^5D_0$ quantum efficiency calculations. For compound Zn−Al−BDC/Eu, the $^5D_0$ quantum efficiency (q), experimental (k_{exp}), radiative (k_r), and nonradiative (k_{nr}) transition probabilities were estimated as 7.7%, 5.025 ms^{-1}, 0.389 ms^{-1}, and 4.636 ms^{-1}, respectively. The nonradiative transition probability is 12 times higher than the radiative one, thus contributing to the small $^5D_0$ quantum efficiency. The higher nonradiative transition probability can be ascribed to the presence of OH oscillators in the form of coordinated water molecules, in agreement with the EXAFS results.

(17) Evans, J.; Gauntlett, J. T.; Mosselmans, J. F. W. *Faraday Discuss. Chem. Soc.* **1990**, 107.
(18) Carlos, L. D.; Messaddeq, Y.; Brito, H. F.; Sá Ferreira, R. A.; de Zea Bermudez, V.; Ribeiro, S. J. L. *Adv. Mater.* **2000**, *12*, 594.
(19) Werts, M. H. V.; Jukes, R. T. F.; Verhoeven, J. W. *Phys. Chem. Chem. Phys.* **2002**, *4*, 1542.

Scheme 1. Preparation of Zn−Al−BDC/Eu, Showing the Proposed Coordination Environment of Eu^{3+} Ions within the Interlayer Region

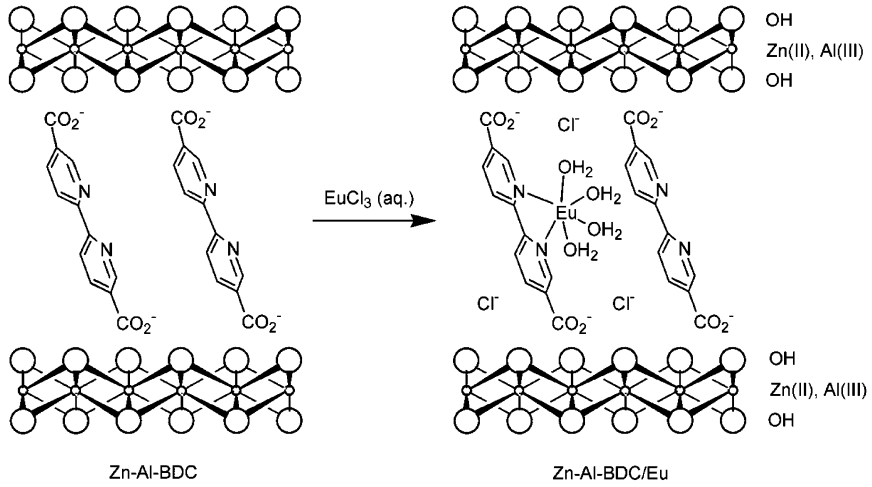

The number of water molecules (n_w) coordinated to the metal ion can be evaluated using the empirical formula suggested by Supkowski and Horrocks:[20]

$$n_w = 1.11 \times [k_{exp} - k_r - 0.31] \quad (4)$$

We can use k_r substituted for the value obtained in D_2O, as originally proposed.[20] The number of water molecules belonging to the Eu^{3+} first coordination sphere in Zn−Al−BDC/Eu was found to be 3.6 ± 0.1. Considering that elemental analysis of this material showed the incorporation of approximately two europium atoms for every three BDC groups (and that the emission spectra show the presence of free BDC ligands), we may deduce that each Eu^{3+} ion is coordinated by two nitrogen atoms from a BDC ligand and four oxygen atoms from water molecules (Scheme 1). This is consistent with the EXAFS results, which indicate a Eu^{3+} coordination number of 7 ± 1.

Conclusion

In this paper, we have shown that a layered double hydroxide pillared by 2,2′-bipyridine-5,5′-dicarboxylate anions is able to chelate lanthanide ions from solution to form intercalated complexes. The photoluminescence results for the europium-containing material show that there is only one type of Eu^{3+} binding site, probably involving 4-coordinated water molecules. Taking into account the EXAFS results, we are led to the conclusion that the europium ions are 6-coordinate, with one bidentate bipyridyl ligand. This is unexpected considering that Eu^{III} complexes are usually 8- or 9-coordinate, although complexes with lower coordination numbers are known. The low coordination number may be due to the fact that the europium ions are confined within a constrained environment. Work is continuing to investigate the chelating abilities of LDH-bipy intercalates and related materials, with the aim of preparing lanthanide-supported hybrids with improved luminescence properties.

Acknowledgment. The authors are grateful to the FCT, OE, and FEDER for financial support (Project POCI//CTM/58507/2004). We acknowledge the European Synchrotron Radiation Facility for provision of synchrotron radiation facilities and would like to thank Dr. Pier Lorenzo Solari for assistance in using beamline BM29. S.G. thanks the University of Aveiro and the FCT for grants. We also wish to thank Prof. João Rocha for access to research facilities and Paula Esculcas for assistance in the NMR experiments.

CM051431P

(20) Supkowski, R. M.; Horrocks, W. DeW., Jr. *Inorg. Chim. Acta* **2002**, *340*, 44.